New $^{40}Ar/^{39}Ar$ dating of the Antrim Plateau Volcanics, Australia: clarifying an age for the eruptive phase of the Kalkarindji continental flood basalt province

Journal Item

Accepted Manuscript

Journal of the Geological Society

New $^{40}Ar/^{39}Ar$ dating of the Antrim Plateau Volcanics, Australia: clarifying an age for the eruptive phase of the Kalkarindji continental flood basalt province

Peter E Marshall, Alison M Halton, Simon P Kelley, Mike Widdowson & Sarah C Sherlock

DOI: https://doi.org/10.1144/jgs2018-035

Received 11 February 2018
Revised 11 July 2018
Accepted 23 July 2018

Supplementary material at https://doi.org/10.6084/m9.figshare.c.4176674

To cite this article, please follow the guidance at http://www.geolsoc.org.uk/onlinefirst#cit_journal

New $^{40}Ar/^{39}Ar$ dating of the Antrim Plateau Volcanics, Australia: clarifying an age for the eruptive phase of the Kalkarindji continental flood basalt province

Peter E. Marshall*[a], Alison M. Halton[b], Simon P. Kelley[c], Mike Widdowson[d], Sarah C. Sherlock[b]

[a]Geotechnics Ltd, Unit 1, Bypass Park Estate, Sherburn in Elmet, North Yorkshire, LS25 6EP, UK.

[b]School of Physical Sciences, The Open University, Walton Hall, Milton Keynes, MK7 6AA, UK.

[c]School of Geosciences, University of Edinburgh, Grant Institute, West Mains Road, Edinburgh, EH9 3JW, UK

[d]Department of Geography, Environment and Earth Sciences, University of Hull, Hull, HU6 7RX, UK.

*Corresponding author:

Dr Peter Marshall

email: petermarshall202@gmail.com

Abstract

The Kalkarindji flood basalt province of northern Australia erupted in the mid-Cambrian. Today the province consists of scattered volcanic and intrusive suites, the largest being the Antrim Plateau Volcanics (APV) in Northern Territory. Accurate dating of Kalkarindji has proved challenging with previous studies focused on minor volcanics and intrusive dykes in Northern Territory and Western Australia. These previously published data, corrected to the same decay constants, range from 512.8-509.6 ± 2.5 Ma [2σ], placing Kalkarindji in apparent synchronicity with the Cambrian Stage 4-5 biotic crisis at 510 ± 1 Ma. This study utilises $^{40}Ar/^{39}Ar$ dating of basalts from the APV to accurately date the major volcanic eruptions in this province. Results yield an age of 508.0-498.3 ± 5.5 Ma [2σ], indicating the APV is younger than the intrusives. These dates allude to a relative timing discrepancy, where intrusive activity in the North Australian Craton preceded the eruption of the APV as the last magmatic activity in the region. The determination of these largest eruptions to be later than 510 Ma, effectively disassociates Kalkarindji lavas from being a major cause of the 510 Ma biotic crisis, but cannot definitively discount any deleterious effects on the fragile Cambrian ecosystem.

Keywords

Kalkarindji; LIP, flood lava volcanism; Ar-Ar dating; multi-stage magmatism; mass extinctions

Large igneous provinces (LIPs), and in particular continental flood basalt provinces (CFBPs), provide an important reference point in geological time due to their significance both as massive, geologically rapid igneous events and their links to environmental change and extinction (Wignall, 2001; Bond and Wignall, 2014). The relationship between CFBPs and mass extinctions has been exhaustively explored by correlating the absolute dating of provinces with the established stratigraphical ages of known mass extinctions through the Phanerozoic (Wignall, 2001; Courtillot and Renne, 2003; Kravchinsky, 2012; Bond and Wignall, 2014). Of the 'big 5' mass extinction events, three can be confidently correlated with CFBPs - Siberian Traps & end Permian, Central Atlantic Magmatic Province (CAMP) & end Triassic, and Deccan Traps & end Cretaceous - whilst the two older events (end Ordovician and Late Devonian) do not yet have such a compelling body of evidence. Although recent studies have speculated on these correlations using Hg as a tracer for LIP volcanism (Jones et al., 2017; Racki et al., 2018). Courtillot and Renne (2003) also identified other significant extinction events that appear to correlate with CFBPs such as the end Guadalupian extinction and the Emeishan flood basalt province, whilst smaller provinces, like Columbia River Basalt Province appear to have had little to no environmental impact (Bond and Wignall, 2014).

Kalkarindji is the oldest CFBP in the Phanerozoic, having erupted onto the North Australian Craton during the mid-Cambrian. Previous dating of samples associated with the Kalkarindji CFBP has demonstrated synchronicity with the Early - Middle Cambrian (EMC; stage 4-5) biotic crisis dated at 510 ± 1 Ma (Jourdan et al., 2014). However, correlation does not equate to causation, yet the LIP and extinction link has been strongly implied.

Debate continues as to whether volatile release from CFBPs into the atmosphere is an effective kill mechanism (Self et al., 2008; Bond and Wignall, 2014; Schmidt et al., 2016). Total period of eruption, pulsed or continuous eruptions, and the buffering of the atmosphere are the main discussion points around whether CFBPs are able to overload the atmosphere to deliver a toxic amount of volatiles into the biotic system. For example, a CFBP with a short total period that comprised continuous

eruptions may have a larger effect on the environment than a longer total period with pulsed eruptions. This scenario depends upon the ability of the atmosphere to recover after each small pulse, but may be unable to buffer against a continuous influx of toxic volatiles and thus be overcome. Recent studies of the Deccan argue for paroxysmal pulses shorter than 1 Myr, based upon high-resolution palaeomagnetic and radiometric dating techniques (Chenet et al., 2008, 2009; Renne et al., 2015; Schoene et al., 2015). This rapid time period is well studied in the Mesozoic - Cenozoic (Courtillot and Renne, 2003; Jerram and Widdowson, 2005) and is dependent on the precision of the adopted dating technique. The accurate dating of Kalkarindji (Hanley and Wingate, 2000; Glass and Phillips, 2006; Evins et al., 2009; Jourdan et al., 2014) extends this record in the Phanerozoic as part of an increase in the dating of ancient CFBPs in the last decade (Ernst et al., 2008; Ernst, 2014). As most dates for Kalkarindji are from intrusive material, new dating of the extrusive outcrop is needed to clarify an age for the main eruptive phase of magmatism and improve our understanding of any LIP - mass extinction link in the early Phanerozoic.

Geology of Kalkarindji CFBP

The Kalkarindji CFBP consists of five individual extrusive sub-provinces extending semi-continuously across Western Australia (WA), Northern Territory (NT) and NW Queensland (Glass and Phillips, 2006) and several geochemically correlated dykes in Western Australia (Hanley and Wingate, 2000; Macdonald et al., 2005; Jourdan et al., 2014) (Fig. 1). In total these outcrops cover an estimated 55,000 km^2 (Bultitude, 1972, 1976; Cutovinos et al., 2002) and would have had an estimated areal extent of ~ 400,000 km^2 (Veevers, 2001), and a volume of ~1.5 x 10^5 km^3 (Glass and Phillips, 2006) as a single connected lava field, potentially making this LIP comparable in size and volume to the well preserved Columbia River Basalt Province, USA (Coffin and Eldholm, 1994; Bryan et al., 2010).

The Antrim Plateau Volcanics (APV), the largest sub-province cropping out over a semi-continuous area of c. 50,000 km^2 in NT and WA, with a maximum lava pile thickness of 1.1 km (Mory and Beere,

1988; Cutovinos et al., 2002) is composed of mainly undifferentiated aphyric basaltic andesite with four minor, recognisable members contained within the basalt pile: the Blackfella Rockhole Member, Bingy Bingy Basalt Member, Mt Close Chert and Malley Springs Sandstone members (Mory and Beere, 1985; Cutovinos et al., 2002; Marshall et al., 2016). The intercalated sediment members occur in localised areas of the province and cannot be considered stratigraphically important, besides indicating periods of volcanic repose and marine/lacustrine inundation of the lava pile. Unconformably underlying the volcanics are a series of Proterozoic quartz to arkosic sandstone basin units and Archean basement fragments of the North Australian Craton (Sweet et al., 1974a, 1974b; Scott et al., 2000). The APV can be split into two 'limbs' - a thin (up to 200 m thick) eastern limb and a thicker (up to 1.1 km thick) western limb (Fig. 1). The vast majority of lava flows ranging from 5 – 50 m thickness, are seen to be near flat-lying and have been subject to little to no tectonic influence.

Previous geochronology

Recent radiometric dating indicates that the Kalkarindji basalts erupted in the mid-Cambrian, with a spread of ages derived from different outcrops and via different methods (Bultitude, 1972; Hanley and Wingate, 2000; Macdonald et al., 2005; Glass and Phillips, 2006; Evins et al., 2009; Jourdan et al., 2014). The initial comprehensive geological mapping of the Antrim Plateau and surrounding sub-provinces by Bultitude (1971, 1972) and Sweet et al. (1971, 1974a, 1974b) provided the first absolute dating of the province through K-Ar geochronology, yielding ages of 500 ± 12 Ma and 511 ± 12 Ma (Bultitude, 1972), attributed to samples collected from the minor satellite provinces of the Nutwood Downs Volcanics and Helen Springs Volcanics, respectively (Fig. 1). The first robust date in 30 years was produced from zircons collected from the doleritic Milliwindi Dyke in the north west Kimberley region (Hanley and Wingate, 2000). This initial zircon $^{207}Pb^*/^{206}Pb^*$ date (513 ± 12 Ma, 95% confidence), is only the third ever reliable date; but whilst this was from an outcrop geochemically indistinct from the Antrim Plateau Volcanics and thus considered part of the greater

Kalkarindji CFBP (Glass and Phillips, 2006), it is nevertheless separated from the extrusive succession by the Halls Creek and King Leopold Orogenic belts. This date was later corroborated by a second U-Pb SHRIMP zircon date (508.0 ± 5.0 Ma, 95% confidence) measured on zircons from the Boondawari Fm - a series of dolerite dykes cutting through the Officer Basin in Western Australia (Macdonald et al., 2005). The Macdonald et al. sample is linked to Kalkarindji based upon the coincidence of the ages of the two Western Australian dolerites only.

For ease of comparison between published dates and samples of this study, all $^{40}Ar/^{39}Ar$ ages have here been recalibrated to the constants defined by Min et al. (2000) and the standard values calculated by Renne et al. (2010) (Table 1). Glass and Phillips (2006) conducted the first $^{40}Ar/^{39}$ Ar dating of the Kalkarindji through the collection of plagioclase bearing samples at one location in the SW of the Antrim Plateau Volcanics producing an age plateau at 509.9 ± 2.2 Ma; reported at 2σ (*LB011*) and a second sample from the Helen Springs Volcanics, which produced reliable plateaux at 512.8 ± 1.6 Ma; 2σ (*HS002(1)*) and 511.3 ± 2.0 Ma; 2σ (*HS002(2)*). Evins et al. (2009) investigated the Table Hill Volcanics, linking this small extrusive lava outcrop in southern Western Australia (Grey et al., 2005) to Kalkarindji through a matching of the geochemical signature and an $^{40}Ar/^{39}Ar$ age of 509.6 ± 2.5 Ma; 2σ. Jourdan et al. (2014) used $^{40}Ar/^{39}Ar$ dating calibrated to Renne et al. (2011), paired with new U-Pb mineral dating to precisely place the province at 510 - 511 Ma. After corrections and homogenised calibration to the most recently determined decay constants most dates of material associated with the Kalkarindji cluster around 510 Ma (Fig. 2).

However, Jourdan et al. re-dated the exact same zircon samples from Hanley and Wingate (2000), dolerite dykes in the Officer Basin and a new found dyke in the Canning basin, all intrusive bodies in Western Australia with presumed relationships to the APV. These ages, these authors propose, makes the Kalkarindji CFBP synchronous with the EMC at 510 ± 1 Ma. (Landing et al., 1998; Harvey et al., 2011; Jourdan et al., 2014). This boundary represents the first significant biotic turnover in the fossil record (~ 45 % of all genera became extinct; Keller, 2005) following the onset of the Cambrian

explosion at c. 542 Ma (Bowring et al., 2007; Maloof et al., 2010). Crucially, all but one of these dates represent the age of intrusives and small volcanic outliers in the Kalkarindji province and should not necessarily be interpreted as fully representative of the province as a whole. Whilst it has been proven that intrusive magmatism may play a larger role than previously thought in producing deleterious environmental effects when intruded into volatile rich sediments (Burgess et al., 2017; Heimdal et al., 2018), the quartzite and arkosic sandstone units in the cratonic basement underlying Kalkarindji point toward voluminous effusive eruptions as the being major contributor to the volatiles released (Self et al., 2005, 2006).

Clearly more data are needed to confidently define any causal relationship between the LIP and biotic crisis, especially samples from the largest volcanic province – the Antrim Plateau Volcanics. Thus, the currently accepted "age" of Kalkarindji is only indicative of an approximate synchronicity to this 'extinction'. Accordingly, this study presents further robust and reliable dates from the APV to accurately date these eruptions.

Rationale and sample selection

One of the key problems in determining accurate $^{40}Ar/^{39}Ar$ dates from the extrusive Kalkarindji volcanics is the paucity of unweathered material. Exposure of the eruptive stratigraphy to tropical, sub-tropical and semi-arid climates for the greater part of the Phanerozoic has resulted in extreme pervasive weathering and profound mineral alteration at outcrop level. In effect, the best materials are either those recovered from intrusive bodies, material from deep boreholes or recently uncovered sections such as road-stone quarries. Whilst intrusive bodies have, so far, yielded promising $^{40}Ar/^{39}Ar$ and U-Pb dates, the precise relationship between these intrusive bodies and the Kalkarindji extrusive lavas (eg. APV) remains unclear.

Samples were selected based on a rigorous test for alteration, their geographic and stratigraphic location within the APV, and their abundance of plagioclase phenocrysts. Two samples were selected from the base of a borehole (BMR Limbunya 1 - LB1; Bultitude, 1971) and three others from surface samples collected during the 2012 field season from an abandoned quarry (VCAQ), a newly uncovered river cutting (BTDF), and from the Bingy Bingy Basalt Member atop a mesa (NLBT), which is in close proximity to, and in the same formation as the LB011 sample analysed by Glass and Phillips (2006).

Determining the degree of alteration

All samples collected during the 2012 field season were tested for their suitability for geochronology using two methods. Firstly samples were analysed by whole-rock XRF at the Open University (Table S2)and assessed using two alteration indices - the chemical index of alteration (CIA - Nesbitt and Young, 1982) and mafic index of alteration (MIA - Babechuk et al., 2014). The MIA builds upon the CIA index through the addition of the mafic mineral constituent elements Fe and Mg. The MIA aims to address the lack of sensitivity in other indices to more mafic parent rocks such as basalt and basaltic andesites and can be used in either oxidising (MIA_O) or reducing (MIA_R) conditions. Figure 3 shows that in all three of these indices, unweathered rocks ae considered to be those which plot with low index numbers, commonly < 50. Unhelpfully, the majority of samples from the APV plot in the unweathered portion (< 50) on all three indices, despite weathering effects such as desert rind and discolouration being obvious in hand sample.

To discriminate further, petrography was utilised to identify nuances within the crystal structure. However, alteration in a petrographic sense is a subjective quality and thus difficult to define and quantify. It is often obvious that a rock has undergone alteration, but to what degree is dependent upon the observer and their understanding of a fresh sample for comparison. Therefore a relative

scale between samples is often the easiest way to describe alteration in a sample set. In this study samples were systematically analysed by microscopy and assigned a score on a relative ten-point scale which allows for the variability of mineral alteration to be assessed and a value determined through three main factors: modal mineralogy, quality of crystal boundaries, and the amount of mineral fracturing and leaching (photomicrographs and geochemical data of samples can be found in supplementary material). Samples were then ranked according to three factors: low alteration score, geographical location, and stratigraphic position. From this ranking, five samples with a greater abundance of plagioclase phenocrysts were chosen for geochronological analysis.

The highest ranked samples were those from the base of BMR Limbunya 1 (LB1) borehole. With a low alteration score based on their crisp crystal boundaries, abundance of primary unaltered plagioclase and a lack of secondary mineral growth, paired with low LOI values and low CIA and MIA index values, highlights the freshness of these samples. These samples are seen to be microcrystalline and were analysed by whole rock step-heating. The freshest surface based sample is VCAQ-001, displaying clear albite twinning on plagioclase phenocrysts with little alteration present in thin section. Chemically, it has a low LOI value (0.58 wt.%) and low weathering indices scores.

Analytical techniques

Two different methods were employed to analyse the samples. The flexibility of using laser-based analysis allows for both step-heating of grains and of whole rock samples, as well as *in situ* spot sampling. This is using the same laser, gettering system and mass spectrometer, thus reducing instrument to instrument correlation issues. Some secondary analyses were made using a Nu Instruments Noblesse noble gas spectrometer for sensitivity correlations.

Step-heating

A step-heating methodology was performed through heating the sample with sequentially increasing laser strength until the whole sample is a fused bead, and has thus released all volatile gases. Samples will yield the age of eruption if the rock has been a 'closed system', with respect to Ar diffusion/loss, from the time of crystallisation to measurement; it will have retained all initial Ar and K, thus the age determined at each step should be constant and therefore statistically meaningful, yielding an accurate dating of the eruption (McDougall and Harrison, 2000; Faure and Mensing, 2005). Should the rock have been exposed to weathering or subjected to hydrothermal alteration, minerals will have become altered, introducing the possibility of opening fast diffusion pathways for the release of Ar from the system. In this instance, the Ar in the whole rock becomes variable from mineral to mineral, causing each step in the experiment to be variable depending upon whether the minerals heated are depleted in Ar or not. This open system will typically yield a younger 'apparent age' often with greater analytical errors.

in situ spot sampling

The issue of alteration causing apparent ages can be avoided by *in situ* spot sampling of unaltered grains, using a point source laser to precisely heat an unaltered patch of K-rich phenocryst whilst leaving any altered groundmass untouched. This should in theory produce closed-system results and 'real' dates, however as this method focuses on single spots within grains, the volume of Ar produced is small and so it becomes harder to achieve high precision consistently, thus reducing the likelihood of yielding a statistically meaningful result. A comparison is also drawn between the relatively homogenous groundmass which is very clearly altered and K-rich phenocrysts to assess the level of alteration which affected the phenocrysts.

Analysis methodology

Selected samples were prepared for analysis as either 100 µm thick sections (BTDF-001, NLBT-006, VCAQ-001) or as crushate (LB1-970-975, LB1-955-960). Crushed samples were produced from 100 µm thick sections by broken mortar and pestle into <1mm fractions. Even though these are the least altered samples from the APV, no acid leach was applied owing to the potential to dissolve the available material to untestable quantities. All samples were bathed in acetone and once dry were split into two sets, packed in foils and weighed. Samples were irradiated for 5:34:08 hours in a series of 17 steps from the 16th - 29th July 2013 in the open-pool type 5 MW medium flux reactor at McMaster Nuclear Reactor, McMaster University, Hamilton, Ontario and analysed in batches from 13th November 2013 - 7th March 2014 at the $^{40}Ar/^{39}Ar$ and Noble Gas laboratory at the Open University using an SPI CW 1062 nm infra-red (IR) fibre laser. After passing through a liquid nitrogen trap, extracted gases were cleaned for 5 minutes using two SAES AP-10 getters running at 450°C and a third at room temperature, following which the gases were initially analysed using a MAP 215-50 mass spectrometer. Secondary measurements were made using the same laser and gas clean up system connected to a Nu Noblesse mass spectrometer in single collector mode. Analyses were corrected using a calculated $^{40}Ar/^{36}Ar$ discrimination value of 283 for the MAP-215- 50 and 295 for the Nu Noblesse (using a calibration noble gas mixture of known composition). System blanks were measured before and after every one or two sample analysis steps to check for drift and background interference. Gas clean-up and inlet is fully automated, with measurement of ^{40}Ar, ^{39}Ar, ^{38}Ar, ^{37}Ar, and ^{36}Ar, each for ten scans, and the final measurements are linear extrapolations back to the inlet time. Irradiation flux was monitored using the GA1550 biotite standard with an age of 99.77 ± 0.1 (Renne et al., 2010). Sample J values were calculated by linear interpolation between two bracketing standards, placed between every 10 samples in the irradiation tube.

Results were corrected for ^{37}Ar and ^{39}Ar decay, and neutron-induced interference reactions. The following correction factors were used: $(^{39}Ar/^{37}Ar)_{Ca}$ = 0.00065 ± 0.00000325, $(^{36}Ar/^{37}Ar)_{Ca}$ = 0.000265 ± 0.000001325, and $(^{40}Ar/^{39}Ar)_{K}$ = 0.0085 ± 0.0000425; based on analyses of Ca and K salts. Ages were calculated using the atmospheric $^{40}Ar/^{36}Ar$ ratio of 298.56 (Lee et al., 2006) and decay

constants of Renne et al. (2010). All data corrections were carried out using bespoke data-reduction software and ages were calculated using Isoplot 4.15 (Ludwig, 2009).

Plateau ages derived from step-heating are defined as a statistically consistent sequence - a plateau of at least three successive incremental steps, incorporating > 60 % ^{39}Ar to give an age concordant at 2σ (or 95 %) confidence level. ^{40}Ar/^{39}Ar results are summarised in Tables 2 and 3, all errors on final ages are quoted at 2σ or 95% confidence and include a 0.5% error on the J value (full data in supplementary material). Graphical data for each sample is presented as either a cumulative age spectra or weighted average plot depending upon whether the analysis was step-heated or spot sampled (Fig. 4). Inverse isochron correlation diagrams, where ^{36}Ar/^{40}Ar is plotted against ^{39}Ar/^{40}Ar, are also calculated (Fig 5).

Initially two samples (LB1-955-960 & LB1-970-975) with a relatively unaltered microcrystalline groundmass were step-heated as whole-rock and the other 3 samples were analysed by the *in situ* spot sampling method using the MAP. Following initial analysis, a secondary set of all 5 samples were step-heated and measured using the more sensitive Nu Noblesse in single collector mode. Data was collected from 3 of 5 secondary samples but none achieved strict plateau criteria of three or more concurrent steps, within error, contributing > 60 % ^{39}Ar. The level of precision of this instrument meant that the error on each step was reduced, decreasing the concordance between them, and thus, no statistical plateaux were achieved, even though the secondary data appears to corroborate with the primary data. However, isochrons produced by this secondary data revealed significant statistics to reaffirm the original data. The two failed samples (BTDF-001(2) and NLBT-006(2)) yielded very high quantities of gas, enough to overwhelm the highly sensitive Noblesse making analysis difficult. These were re-analysed by step heating using the MAP 215-50 system, resulting in a total of 10 ^{40}Ar/^{39}Ar analyses.

Results

LB1-970-975

Both analyses from this sample yield ages within error of one another. The plateau from analysis (1) used 70% of available ^{39}Ar, producing an age of 508.0 ± 8.1 Ma (2σ; MSWD: 0.4; p = 0.88). The isochron data produces a slightly older age at 512.9 ± 7.1 Ma (MSWD: 1.8; p = 0.07) with an initial $^{40}Ar/^{36}Ar$ estimate (336 ± 19) which is slightly elevated above atmospheric ratio of 298.56, yet is well within error of the plateau age. This enlarged error and low probability may be due to the clumping of data near to 0 on the y-axis. The secondary analysis did not produce a statistical plateau due to the increased precision of the Nu Noblesse, however the apparent spread of data on the inverse isochron allows for an accurate initial $^{40}Ar/^{36}Ar$ estimate (295 ± 15), thus the age produced (497.9 ± 7.5 Ma; MSWD: 25; p = 0.00) can accepted - this is within error of the primary analysis. A weighted average of these two analyses is 502.6 ± 5.5 Ma (2σ; MSWD: 3.3; p = 0.07).

LB1-955-960

Both analyses from this sample agree. The plateau age of 499.8 ± 7.0 Ma (2σ; MSWD: 1.6; p = 0.15) using 95.3 % of ^{39}Ar from analysis (1) is in agreement with the inverse isochron age of 498.6 ± 7.0 Ma (MSWD: 1.4; p = 0.20) with a good spread of data, despite some clumping of error ellipses, producing an initial $^{40}Ar/^{36}Ar$ estimate of 325 ± 25. The secondary analysis again doesn't reach plateau due to smaller error on individual steps. The spread of data along the isochron again produces an accurate initial $^{40}Ar/^{36}Ar$ estimate (298 ± 16) and thus an accepted age (496.9 ± 6.6 Ma; MSWD: 20; p = 0.00) within error of the primary analysis. A weighted average of these two analyses is 498.3 ± 4.8 Ma (2σ; MSWD: 0.36; p = 0.55).

BTDF-001

BTDF-001(1) spot samples produce a weighted average of 511.3 ± 5.7 Ma (2σ with 0/16 rejections; MSWD: 1.5; p = 0.09) with an inverse isochron in agreement within error (508.9 ± 8.2 Ma; MSWD: 1.6; p = 0.07), with a good spread of data producing an accurate initial $^{40}Ar/^{36}Ar$ estimate of 302 ± 10. BTDF-001(2) is a step-heated analysis producing a plateau at 505.3 ± 6.6 Ma (2σ; MSWD: 1.7; p = 0.08) with 95.2% of ^{39}Ar used. The inverse isochron for this analysis suffers from extensive clumping of data at 0 on the y-axis, thus with little spread in the data this initial $^{40}Ar/^{36}Ar$ ratio of 403 ± 51 is unreliable. However, as this secondary sample is well within error of the primary sample both can be classed as internally repeatable and thus accepted. A weighted average of these two analyses is 508.7 ± 4.3 Ma (2σ; MSWD: 1.9; p = 0.17).

VCAQ-001

Spot samples on VCAQ-001(1) produce a weighted average of 517.6 ± 7.6 Ma (2σ with 2/16 points rejected; MSWD: 0.99; p = 0.46). The inverse isochron of this data produces an age of 520.4 ± 56 Ma (MSWD: 4.4; p = 0.00) with an initial $^{40}Ar/^{36}Ar$ estimate of 317 ± 74. These large errors are attributed to the large inherent error ellipses in the isochron. The secondary analysis, conducted on the Nu Noblesse did not produce a plateau, but an isochron age of 490.2 ± 7.7 Ma (MSWD: 4.5; p = 0.00) and an initial $^{40}Ar/^{36}Ar$ ratio of 326 ± 15 results from a small spread in the data, the majority are clumped together. The large error in the primary analysis and the lack of internal precision discounts both analyses from this sample.

NLBT-006

NLBT-006(1) spot samples produce a weighted average age of 411.0 ± 22 Ma (95% with 0/18 rejections; MSWD: 9.5; p = 0.00). The inverse isochron produces an age of 441.0 ± 55.0 Ma (MSWD: 9.8; p = 0.00) with an initial $^{40}Ar/^{36}Ar$ estimate of 280 ± 19. The large errors on these data are caused by the lack of samples at the base of the $^{40}Ar/^{36}Ar$ extrapolation. The secondary step-heated sample, NLBT-006(2), yielded an age of 470.5 ± 8.5 Ma (2σ; MSWD: 1.11; p = 0.35) from 100% of ^{39}Ar and an isochron age of 469.0 ± 9.1 Ma (MSWD: 1.2; p = 0.26) with an initial $^{40}Ar/^{36}Ar$ estimate of 304 ± 26. Whilst this secondary sample appears to be statistically sound, large error ellipses in the isochron mean that the extrapolation could be skewed away from its current position and still be 'accurate'. The initial steps of the analysis are included even though their error are large, thus reducing the accuracy of the overall plateau. Although this age is possibly a reasonable estimate for the age of this sample it if of low precision; these issues, paired with the lack of internal precision between analyses (1) and (2) discount this sample.

Discussion

Age of the Antrim Plateau Volcanics

The three positive results (498.3 ± 4.8 Ma, 502.6 ± 5.5 Ma and 508.7 ± 4.3 Ma) from this study add to the single age garnered from LB011 (509.9 ± 2.2 Ma; Glass and Phillips, 2006) to quadruple the meaningful ages from the Antrim Plateau Volcanics (Table 4), and extend the data for Kalkarindji as a whole to 14 data points (Fig. 6). This is still a very small dataset when compared with more well-known CFB provinces such as the Deccan (Pande et al., 2017; Subbarao and Courtillot, 2017), which shows the work still to be done to improve upon the accuracy of the age of Kalkarindji to better understand the nuances and complexities of the geodynamics of this CFBP. The dates of this study do give us a slight peek into the possible evolution and impact of this eruption.

Geographically, the samples from this study are located in the south-west (LB1) and south east (BTDF) of the APV, giving an agreement across the two 'limbs' of the province, indicating an eruption duration across the whole province which is shorter than statistical error can account for.

The two samples from the base of the borehole yield ages of ~5 Myrs younger than the two samples obtained at the ground level (LB011 & BTDF-001), although these are within error. This could perhaps indicate a very rapid eruption, shorter than the inherent error associated with Ar dating, or the more likely scenario that the surface samples have undergone a small degree of previously unidentified alteration, introducing excess argon into the system.

Effects of alteration

The age of a sample determined by $^{40}Ar/^{39}Ar$ analysis can appear erroneous to an expected date (as constrained by independent relative and absolute dating methods) owing to several factors which may have affected closure of the Ar system post emplacement. The system is most notably affected by the influence of diagenetic fluids passing through the rock, leaching elements from minerals and re-depositing them as secondary clay minerals. Potassium bearing fluids have the potential to elevate K in a sample, increasing the ^{39}Ar content (daughter product of ^{39}K during irradiation) and lowering the $^{40}Ar/^{39}Ar$ ratio; thus the sample will yield apparently younger ages. If fluids are depleted in K, leaching will occur, reducing the ^{39}K content, resulting in an artificially elevated $^{40}Ar/^{39}Ar$ ratio and an apparently older age. These scenarios assume the ^{40}Ar content remains constant and is unaffected by alteration. In reality, the introduction of fluids will most likely release Ar contained within minerals, reducing the ^{40}Ar content and yielding younger apparent ages. However, when the fluids are Ar-bearing, excess argon ($^{40}Ar_E$) is introduced by diffusion into the mineral or melt inclusions (Kelley, 2002). The presence of $^{40}Ar_E$ is monitored by the $^{40}Ar/^{36}Ar$ ratio in comparison with the known atmospheric ratio of 298.56 (Lee et al., 2006). ^{39}Ar recoil may also be a problem to

encounter with spot sampling as this affects individual crystals. It is likely to be seen in the altered matrix groundmass and early low-temperature phases of step-heating. However, although recoil is likely in all potassium bearing samples, redistribution of ^{39}K by diagenetic fluids is likely to be the overwhelming factor behind erroneous ages.

The two samples that were discounted have not produced meaningful ages due to a variety of reasons. VCAQ-001(1), produced a weighted average age at 517.6 ± 7.6 Ma, but incurred very large errors on the isochron, attributed to the spread of ellipses along the regression line. There is no cluster at 0 on the y-axis, instead seen around 0.0005 as a loose cluster of relatively large ellipses, indicating a loss in radiogenic Ar from this sample. Whilst no plateau was forthcoming from VCAQ-001(2) the isochron should record an older age, with a relatively high MSWD of 4.5 and initial $^{40}Ar/^{36}Ar$ intercept at 326 ± 15, but is instead younger, indicating a loss in radiogenic argon and an influence of alteration through the sample.

NLBT-006(1) yielded a young age of 411.0 ± 22.0 Ma from spot sampling with large error on this and the isochron age (441.0 ± 55 Ma). These errors are attributed to the diagenesis which is likely to have occurred. The $^{37}Ar/^{39}Ar$ ratio can be used as a proxy for the Ca/K ratio of a sample to monitor alkali movement. In NLBT-006 this ratio is reduced compared to whole-rock data (< 5.1). This is explained by the preferential weathering to have affected plagioclase in these samples, whereby Ca is lost through saussuritization in plagioclase (Marshall, 2015), thus relatively increasing the ^{39}K present, and inducing an artificially young age. The isochon on NLBT-006(2) relies on large data-point ellipses with large error, indicating the isochron to be intrinsically flawed; the line of best fit could be moved significantly and still fit the ellipses, thus changing the date and initial $^{40}Ar/^{36}Ar$ value without changing the data.

Dates produced in this study indicate that both spot sampling and step-heating can produce both statistically reliable and 'apparent' ages. Due to the stepped nature of step-heating, this method is able to identify the presence of Ar_E and ^{39}Ar recoil and how they vary through the experiment. These

are usually released in the early low temperature steps, as seen in LB1-970-975(1) and LB1-955-960(1). However, where alteration is more pervasive the error on each step may be large enough to skew the plateau as seen in NLBT-006(2). With spot sampling, a good age depends upon the precision of the analysis, indicated by the repeatability of the ages yielded (Fig. 4). High precision on fresh samples yields good dates (BTDF-001(1)), whereas, if precision is low this can yield erroneous ages (VCAQ-001(1) & NLBT-006(1)), thus a weighted average becomes skewed. To improve upon this, a time consuming picking procedure can be undertaken to pick the cleanest and freshest plagioclase crystals. However, as seen with many Kalkarindji samples, alteration is affecting crystals from their inside and may not be visible in a picking procedure. To avoid this particular problem, an acid leach could have been applied to crystals, removing sericite and other alteration products from the original material. However, it was determined that an acid leach on altered samples such as these from the Kalkarindji, had the potential to dissolve the available material to practically zero, hence no leach was applied during this study.

Multiple stages of magmatism

The most reliable dates offered by previous authors represent intrusive bodies from the Canning Basin (511 ± 5 Ma), Officer Basin (511 ± 4 Ma) and Milliwindi Dyke (510.7 ± 0.6 Ma - Jourdan et al., 2014); and small volcanic outliers in the Table Hill Volcanics (509.6 ± 2.5 Ma - Evins et al., 2009) and Helen Springs Volcanics (512.1 ± 1.8 Ma - Glass and Phillips, 2006). Importantly, there has been only a single successful date from the Antrim Plateau Volcanics (509.9 ± 2.2 Ma - Glass and Phillips, 2006). Compared to these previous dating attempts of the province which, when corrected to the same decay constant, range from 512.8 - 509.6 ± 2.5 Ma, the new dates of this study are significantly younger at 508 - 498 ± 5 Ma. This discrepancy between the different ages and their geographical placement leads to a new hypothesis for the magmatic evolution of the Kalkarindji province. The oldest dates indicate the early onset of intrusive magmatism into the Western Australian cratons

between 512 - 510 Ma. Smaller satellite provinces are found to erupt first between 512 - 509 Ma before the main volcanic expression of the Antrim Plateau erupted between 508 - 498 Ma.

This leads to new interpretations regarding the EMC biotic crisis at 510 Ma and the impact that Kalkarindji had on the Cambrian environment. With the biotic turnover dated to 510 ± 1 Ma, it follows that for the CFBP to have been a significant factor in the environmental decay which led to this extinction, the initial input of volatiles must have been synchronous with the established extinction marker layer (Wignall, 2011). As the early Cambrian biota, having never been witness to significant environmental change before, may not have been resilient enough to survive the slightest changes, it is conceivable that the intrusives in Western Australia may be linked to the EMC in a similar fashion to the Siberian Traps (Burgess et al., 2017), although confirmation of this requires further investigation into the volatile content of the specific units intruded. However, the Antrim Plateau Volcanics are too young to be a factor with this biotic crisis (Fig. 6), with previous studies of emissions from Kalkarindji suggesting that these eruptions were unlikely to have caused any significant impact on the atmospheric compositions at that time (Marshall et al., 2016). This is not to say that Kalkarindji did not cause any environmental change, previous C-isotope excursion studies in the mid-late Cambrian show significant changes were occurring in this period (Fan et al., 2011).

Significant swings between positive and negative excursions in the Cambrian carbon curve (Fig. 6) show that the global carbon cycle was rapidly adapting with the advent of new biota and ecosystems, and that it would have been particularly susceptible to a range of forcing factors (Faggetter et al., 2017). For instance, the sudden release of large amounts of CH_4 or CO_2 to the atmosphere, has the potential to affect the positive and negative feedbacks between all of the Earth's major domains (the atmosphere, biosphere, lithosphere, and hydrosphere). Indeed, notable and well-documented $\delta^{13}C$ excursions later in the Phanerozoic may be effected by factors including eustatic and climate change, clathrate release, bolide impact and LIP volcanism (Doney and Schimel, 2007; Zachos et al., 2008). Acidification of seawater and increased rates of continental weathering

are two consequences of global warming forced by substantial and abrupt increases in the level of atmospheric CO_2; such releases can be achieved through large-scale volcanism and the subsequent environmental changes continued for many tens or hundreds of thousands of years after their start (Wignall et al., 2009; Dickson et al., 2012). However, Marshall et al. (2016) discussed the effectiveness of an equatorial CFBP eruption during the Cambrian, indicating that whilst this location is favourable for aerosol distribution into both hemispheres, the eruption column needs to penetrate the high tropopause to have worldwide influence. Whether the Kalkarindji lavas were sufficiently extensive and potent enough to have contributed to a major environmental catastrophe requires further investigation.

Conclusions

The age of Kalkarindji and its geological history post-emplacement has resulted in a greater degree of alteration of samples than initially expected. Of the 5 samples selected for analysis, two have provided unreliable data yielding apparent ages due to reasons associated with this pervasive alteration. Three samples, 1 from surface locations and 2 from the base of the BMR Limbunya 1 borehole have yielded reliable, statistically confident ages which agree, within error, with each other and previously published data, although the APV samples are clearly younger than the intrusives and satellite provinces of Kalkarindji.

The coincidence of age between BTDF-001 and LB011 and the divergence between these and the samples from LB1 could indicate that surface samples have undergone a slight gain in argon in comparison to those from lower in the stratigraphy. The discrepancy with ages yielded by some previous studies may be explained by the fact that these have dated different expressions of the broader 'magmatic event'; all may have the same geochemistry, but most are intrusive dykes or else satellite provinces to the main APV. We therefore suggest that the APV was erupted after these

dykes and outer provinces were emplaced. Consequently, if these new dates are correct and the timing of the APV is discordant from other dated outcrops of Kalkarindji, the largest expression of basalt in the province was most likely to have erupted after the 510 Ma biotic crisis. Nevertheless, if the main Kalkarindji extrusive phase can be thus discounted as being a major cause of this particular environmental change, it would not discount it from having triggered environmental change later in the Cambrian.

Acknowledgements and Funding

This research was conducted at the Open University and funded by a joint PhD grant from the Open University and Proto Resources & Investments Ltd awarded to P. Marshall. Samples were collected in 2012 by P. Marshall, M. Widdowson, L. Faggetter & B. Gray. We are indebted to the landowners and tenants of stations in Northern Territory, in particular S. Craig for access to key locations on Nelson Springs cattle station. Geoscience Australia are thanked for access to BMR archives. D. Murphy, S. Blake, S. Gibson and D. Phillips are thanked for their insightful comments and discussion on improving this manuscript. Constructive reviews to enhance this manuscript further from C. Sprain and two anonymous reviewers are gratefully acknowledged.

Appendices

See Supplementary Material for $^{40}Ar/^{39}Ar$ analysis data tables, XRF geochemical data, alteration study and photomicrographs of all 5 samples.

References

Babechuk, M.G., Widdowson, M., Kamber, B.S. (2014). Quantifying chemical weathering intensity and trace element release from two contrasting basalt profiles, Deccan Traps, India. *Chem.*

Geol. **363**, 56–75. https://dx.doi.org/10.1016/j.chemgeo.2013.10.027.

Bond, D.P.G., Wignall, P.B. (2014). Large igneous provinces and mass extinctions: An update. *Geol. Soc. Am. Spec. Pap.* **505**, 29–55. https://dx.doi.org/10.1130/2014.2505(02).

Bowring, S.A., Grotzinger, J.P., Condon, D.J., Ramezani, J., Newall, M.J., Allen, P.A. (2007). Geochronologic constraints on the chronostratigraphic framework of the neoproterozoic Huqf Supergroup, Sultanate of Oman. *Am. J. Sci.* **307**, 1097–1145. https://dx.doi.org/10.2475/10.2007.01.

Bryan, S.E., Ukstins Peate, I., Peate, D.W., Self, S., Jerram, D.A., Mawby, M.R., Marsh, J.S. (Goonie) S.G., Miller, J.A. (2010). The largest volcanic eruptions on Earth. *Earth-Science Rev.* **102**, 207–229. https://dx.doi.org/10.1016/j.earscirev.2010.07.001.

Bultitude, R.J. (1971). The Antrim Plateau Volcanics, Victoria River District, Northern Territory. *Bur. Miner. Resour. Geol. Geophys.* **1971/69**.

Bultitude, R.J. (1972). The Geology and Petrology of the Helen Springs, Nutwood Downs, and Peaker Piker Volcanics. *Bur. Miner. Resour. Geol. Geophys.* **1972/74**.

Bultitude, R.J. (1976). Flood basalts of probable early Cambrian age in northern Australia, in: Johnson, R.W. (Ed.), *Volcanism in Australasia*. Canberra, pp. 1–20.

Burgess, S.D., Muirhead, J.D., Bowring, S.A. (2017). Initial pulse of Siberian Traps sills as the trigger of the end-Permian mass extinction. *Nat. Commun.* **8**, 1–4. https://dx.doi.org/10.1038/s41467-017-00083-9.

Chenet, A.-L., Fluteau, F., Courtillot, V., Gérard, M., Subbarao, K. V. (2008). Determination of rapid Deccan eruptions across the Cretaceous-Tertiary boundary using paleomagnetic secular variation: Results from a 1200-m-thick section in the Mahabaleshwar escarpment. *J. Geophys. Res.* **113**, B04101. https://dx.doi.org/10.1029/2006JB004635.

Chenet, A.L., Courtillot, V., Fluteau, F., Gérard, M., Quidelleur, X., Khadri, S.F.R., Subbarao, K. V., Thordarson, T. (2009). Determination of rapid Deccan eruptions across the Cretaceous-Tertiary boundary using paleomagnetic secular variation: 2. Constraints from analysis of eight new sections and synthesis for a 3500-m-thick composite section. *J. Geophys. Res. Solid Earth* **114**, 1–38. https://dx.doi.org/10.1029/2008JB005644.

Coffin, M.F., Eldholm, O. (1994). Large igneous provinces: crustal structure, dimensions, and external consequences. *Rev. Geophys.* **32**, 1–36. https://dx.doi.org/10.1029/93RG02508.

Courtillot, V.E., Renne, P.R. (2003). On the ages of flood basalt events. *Comptes Rendus Geosci.* **335**, 113–140. https://dx.doi.org/10.1016/S1631-0713(03)00006-3.

Cutovinos, A., Beier, P.R., Kruse, P.D., Abbott, S.T., Dunster, J.N., Brescianini, R.F., Abbot, S.T., Dunster, J.N., Brescianini, R.F. (2002). *Limbunya, Northern Territory (Second Edition), 1:250 000 geological map series and explanatory notes, SE 52-07*. Northern Territory Geological Survey, Darwin and Alice Springs.

Dickson, A.J., Cohen, A.S., Coe, A.L. (2012). Seawater oxygenation during the Paleocene-Eocene Thermal Maximum. *Geol.* **40**, 639–642. https://dx.doi.org/10.1130/G32977.1.

Doney, S.C., Schimel, D.S. (2007). Carbon and climate system coupling on timescales from the Precambrian to the anthropocene. *Annu. Rev. Environ. Resour.* **32**, 31–66. https://dx.doi.org/10.1146/annurev.energy.32.041706.124700.

Ernst, R.E. (2014). *Large Igneous Provinces*. Cambridge University Press, Cambridge.

Ernst, R.E., Wingate, M.T.D., Buchan, K.L., Li, Z.X. (2008). Global record of 1600–700 Ma Large Igneous Provinces (LIPs): Implications for the reconstruction of the proposed Nuna (Columbia) and Rodinia supercontinents. *Precambrian Res.* **160**, 159–178. https://dx.doi.org/10.1016/j.precamres.2007.04.019.

Evins, L.Z., Jourdan, F., Phillips, D. (2009). The Cambrian Kalkarindji Large Igneous Province: Extent and characteristics based on new $^{40}Ar/^{39}Ar$ and geochemical data. *Lithos* **110**, 294–304. https://dx.doi.org/10.1016/j.lithos.2009.01.014.

Faggetter, L.E., Wignall, P.B., Pruss, S.B., Newton, R.J., Sun, Y., Crowley, S.F. (2017). Trilobite extinctions, facies changes and the ROECE carbon isotope excursion at the Cambrian Series 2-3 boundary, Great Basin, western USA. *Palaeogeogr. Palaeoclimatol. Palaeoecol.* **478**, 53–66. https://dx.doi.org/10.1016/j.palaeo.2017.04.009.

Fan, R., Deng, S., Zhang, X. (2011). Significant carbon isotope excursions in the Cambrian and their implications for global correlations. *Sci. China Earth Sci.* **54**, 1686–1695. https://dx.doi.org/10.1007/s11430-011-4313-z.

Faure, G., Mensing, T.M. (2005). *Isotopes: principles and applications*, 3rd ed. ed. John Wiley & Sons, Inc, Hoboken, New Jersey.

Glass, L.M., Phillips, D. (2006). The Kalkarindji continental flood basalt province: A new Cambrian large igneous province in Australia with possible links to faunal extinctions. *Geology* **34**, 461–464. https://dx.doi.org/10.1130/G22122.1.

Gradstein, F.M., Ogg, J.G., Schmitz, M., Ogg, G. (2012). *The Geologic Time Scale 2012*, 1st ed.

Grey, K., Hocking, R.M., Stevens, M.K., Bagas, L., Carlsen, G.M., Irimies, F., Pirajno, F., Haines, P., Apak, S.N. (2005). *Lithostratigraphic nomenclature of the Officer Basin and correlative parts of the Paterson Orogen, Western Australia*, Geological Survey of Western Australia.

Hanley, L.M., Wingate, M.T.D. (2000). SHRIMP zircon age for an Early Cambrian dolerite dyke: An intrusive phase of the Antrim Plateau Volcanics of northern Australia. *Aust. J. Earth Sci.* **47**, 1029–1040. https://dx.doi.org/10.1046/j.1440-0952.2000.00829.x.

Harvey, T.H.P., Williams, M., Condon, D.J., Wilby, P.R., Siveter, D.J., Rushton, A.W.A., Leng, M.J., Gabbott, S.E. (2011). A refined chronology for the Cambrian succession of southern Britain. *J. Geol. Soc. London.* **168**, 705–716. https://dx.doi.org/10.1144/0016-76492010-031.

Heimdal, T.H., Svensen, H.H., Ramezani, J., Iyer, K., Pereira, E., Rodrigues, R., Jones, M.T., Callegaro, S. (2018). Large-scale sill emplacement in Brazil as a trigger for the end-Triassic crisis. *Sci. Rep.* **8**, 1–12. https://dx.doi.org/10.1038/s41598-017-18629-8.

Ishikawa, T., Ueno, Y., Shu, D., Li, Y., Han, J., Guo, J., Yoshida, N., Maruyama, S., Komiya, T. (2014). The $\delta^{13}C$ excursions spanning the Cambrian explosion to the Canglangpuian mass extinction in the Three Gorges area, South China. *Gondwana Res.* **25**, 1045–1056. https://dx.doi.org/10.1016/j.gr.2013.03.010.

Jerram, D.A., Widdowson, M. (2005). The anatomy of Continental Flood Basalt Provinces: geological constraints on the processes and products of flood volcanism. *Lithos* **79**, 385–405. https://dx.doi.org/10.1016/j.lithos.2004.09.009.

Jones, D.S., Martini, A.M., Fike, D.A., Kaiho, K. (2017). A volcanic trigger for the late ordovician mass

extinction? Mercury data from south china and laurentia. *Geology* **45**, 631–634. https://dx.doi.org/10.1130/G38940.1.

Jourdan, F., Hodges, K., Sell, B., Schaltegger, U., Wingate, M.T.D., Evins, L.Z., Soderlund, U., Haines, P.W., Phillips, D., Blenkinsop, T. (2014). High-precision dating of the Kalkarindji large igneous province, Australia, and synchrony with the Early-Middle Cambrian (Stage 4-5) extinction. *Geology* **42**, 543–546. https://dx.doi.org/10.1130/G35434.1.

Keller, G. (2005). Impacts, volcanism and mass extinction: random coincidence or cause and effect? *Aust. J. Earth Sci.* **52**, 725–757. https://dx.doi.org/10.1080/08120090500170393.

Kelley, S. (2002). K-Ar and Ar-Ar Dating. *Rev. Mineral. Geochemistry* **47**, 785–818. https://dx.doi.org/10.2138/rmg.2002.47.17.

Kravchinsky, V.A. (2012). Paleozoic large igneous provinces of Northern Eurasia: Correlation with mass extinction events. *Glob. Planet. Change* **86**–**87**, 31–36. https://dx.doi.org/10.1016/j.gloplacha.2012.01.007.

Landing, E., Bowring, S.A., Davidek, K.L., Westrop, S.R., Geyer, G., Heldmaier, W. (1998). Duration of the Early Cambrian: U-Pb ages of volcanic ashes from Avalon and Gondwana. *Can. J. Earth Sci.* **35**, 329–338. https://dx.doi.org/10.1139/e97-107.

Lee, J.Y., Marti, K., Severinghaus, J.P., Kawamura, K., Yoo, H.S., Lee, J.B., Kim, J.S. (2006). A redetermination of the isotopic abundances of atmospheric Ar. *Geochim. Cosmochim. Acta* **70**, 4507–4512. https://dx.doi.org/10.1016/j.gca.2006.06.1563.

Ludwig, K.R. (2009). Isoplot 4.15.

Macdonald, F.A., Wingate, M.T.D., Mitchell, K. (2005). Geology and age of the Glikson impact structure, Western Australia. *Aust. J. Earth Sci.* **52**, 641–651. https://dx.doi.org/10.1080/08120090500170419.

Maloof, A.C., Porter, S.M., Moore, J.L., Dudás, F.Ö., Bowring, S.A., Higgins, J.A., Fike, D.A., Eddy, M.P. (2010). The earliest Cambrian record of animals and ocean geochemical change. *Bull. Geol. Soc. Am.* **122**, 1731–1774. https://dx.doi.org/10.1130/B30346.1.

Marshall, P.E. (2015). *The Volcanic Architecture, Geochemistry and Geochronology of the Kalkarindji Continental Flood Basalt Province, Australia*. PhD Thesis. The Open University.

Marshall, P.E., Widdowson, M., Murphy, D.T. (2016). The Giant Lavas of Kalkarindji: rubbly pāhoehoe lava in an ancient continental flood basalt province. *Palaeogeogr. Palaeoclimatol. Palaeoecol.* **441**, 22–37. https://dx.doi.org/10.1016/j.palaeo.2015.05.006.

McDougall, I., Harrison, T.M. (2000). *Geochronology and Thermochronology by the $^{40}Ar/^{39}Ar$ Method*, 2nd ed. Oxford Univ. Press, New York. https://dx.doi.org/10.1093/petrology/41.12.1823.

McDougall, I., Wellman, P. (2011). Calibration of GA1550 biotite standard for K/Ar and $^{40}Ar/^{39}Ar$ dating. *Chem. Geol.* **280**, 19–25. https://dx.doi.org/10.1016/j.chemgeo.2010.10.001.

Min, K., Mundil, R., Renne, P.R., Ludwig, K.R. (2000). A test for systematic errors in $^{40}Ar/^{39}Ar$ geochronology through comparison with U/Pb analysis of a 1.1-Ga rhyolite. *Geochim. Cosmochim. Acta* **64**, 73–98. https://dx.doi.org/10.1016/S0016-7037(99)00204-5.

Mory, A.J., Beere, G.M. (1985). Palaeozoic stratigraphy of the Ord Basin, Western Australia and Northern Territory. *Geol. Surv. West. Aust. Artic.* **14**, 36–45.

Mory, A.J., Beere, G.M. (1988). Geology of the Onshore Bonaparte and Ord Basins in Western Australia. *Geol. Surv. West. Aust. Bull.* **134**, 1–200.

Nesbitt, H.W., Young, G.M. (1982). Early Proterozoic climates and plate motions inferred from major element chemistry of lutites. *Nature* **299**, 715–717. https://dx.doi.org/10.1038/299175a0.

Pande, K., Yatheesh, V., Sheth, H. (2017). 40Ar/39Ar dating of the Mumbai tholeiites and Panvel flexure: intense 62.5 Ma onshore–offshore Deccan magmatism during India-Laxmi Ridge–Seychelles breakup. *Geophys. J. Int.* **210**, 1160–1170.

Racki, G., Rakociński, M., Marynowski, L., Wignall, P.B. (2018). Mercury enrichments and the Frasnian-Famennian biotic crisis: A volcanic trigger proved? *Geology* **46**, 543–546. https://dx.doi.org/10.1130/G40233.1.

Renne, P.R., Balco, G., Ludwig, K.R., Mundil, R., Min, K. (2011). Response to the comment by W.H. Schwarz et al. on " Joint determination of 40K decay constants and 40Ar*/40K for the Fish Canyon sanidine standard, and improved accuracy for 40Ar/39Ar geochronology" by P.R. Renne et al. (2010). *Geochim. Cosmochim. Acta* **75**, 5097–5100. https://dx.doi.org/10.1016/j.gca.2011.06.021.

Renne, P.R., Mundil, R., Balco, G., Min, K., Ludwig, K.R., Mundil, R., Min, K. (2010). Joint determination of ^{40}K decay constants and ^{40}Ar∗/^{40}K for the Fish Canyon sanidine standard, and improved accuracy for ^{40}Ar/^{39}Ar geochronology. *Geochim. Cosmochim. Acta* **74**, 5349–5367. https://dx.doi.org/10.1016/j.gca.2011.06.021.

Renne, P.R., Sprain, C.J., Richards, M.A., Self, S., Vanderkluysen, L., Pande, K. (2015). State shift in Deccan volcanism at the Cretaceous-Paleogene boundary, possibly induced by impact. *Science (80-.).* **350**, 76–78. https://dx.doi.org/10.1126/science.aac7549.

Renne, P.R., Swisher, C.C., Deino, A.L., Karner, D.B., Owens, T.L., DePaolo, D.J. (1998). Intercalibration of standards, absolute ages and uncertainties in ^{40}Ar/^{39}Ar dating. *Chem. Geol.* **145**, 117–152. https://dx.doi.org/10.1016/S0009-2541(97)00159-9.

Schmidt, A., Skeffington, R.A., Thordarson, T., Self, S., Forster, P.M., Rap, A., Ridgwell, A., Fowler, D., Wilson, M., Mann, G.W., Wignall, P.B., Carslaw, K.S. (2016). Selective environmental stress from sulphur emitted by continental flood basalt eruptions. *Nat. Geosci.* **9**, 77–82. https://dx.doi.org/10.1038/ngeo2588.

Schoene, B., Samperton, K.M., Eddy, M.P., Keller, G., Adatte, T., Bowring, S.A., Khadri, S.F.R., Gertsch, B. (2015). U-Pb geochronology of the Deccan Traps and relation to the end-Cretaceous mass extinction. *Science (80-.).* **347**, 182–184. https://dx.doi.org/10.1126/science.aaa0118.

Scott, D.L., Rawlings, D.J., Page, R.W., Tarlowski, C.Z., Idnurm, M., Jackson, M.J., Southgate, P.N. (2000). Basement framework and geodynamic evolution of the Palaeoproterozoic superbasins of north-central Australia: An integrated review of geochemical, geochronological and geophysical data. *Aust. J. Earth Sci.* **47**, 341–380. https://dx.doi.org/10.1046/j.1440-0952.2000.00793.x.

Self, S., Blake, S., Sharma, K., Widdowson, M., Sephton, S. (2008). Sulfur and chlorine in late Cretaceous Deccan magmas and eruptive gas release. *Science (80-.).* **319**, 1654–7. https://dx.doi.org/10.1126/science.1152830.

Self, S., Thordarson, T., Widdowson, M. (2005). Gas Fluxes from Flood Basalt Eruptions. *Elements* **1**, 283–287. https://dx.doi.org/10.2113/gselements.1.5.283.

Self, S., Widdowson, M., Thordarson, T., Jay, A.E. (2006). Volatile fluxes during flood basalt eruptions and potential effects on the global environment: A Deccan perspective. *Earth Planet. Sci. Lett.* **248**, 518–532. https://dx.doi.org/10.1016/j.epsl.2006.05.041.

Subbarao, K. V, Courtillot, V. (2017). Deccan basalts in and around Koyna — Warna region, Maharashtra: Some reflections. *J. Geol. Soc. India* **90**, 653–662. https://dx.doi.org/10.1007/s12594-017-0772-y.

Sweet, I.P., Mendum, J.R., Bultitude, R.J., Morgan, C.M. (1971). The Geology of the Waterloo, Victoria River Downs, Limbunya and Wave Hill 1:250,000 Sheet Areas, Northern Territory. *Bur. Miner. Resour. Geol. Geophys.* **1971/71**.

Sweet, I.P., Mendum, J.R., Bultitude, R.J., Morgan, C.M. (1974a). The Geology of the Southern Victoria River Region, Northern Territory. *Bur. Miner. Resour. Geol. Geophys.* **Report 167**.

Sweet, I.P., Mendum, J.R., Morgan, C.M., Pontifex, I.R. (1974b). The Geology of the Northern Victoria River Region, Northern Territory. *Bur. Miner. Resour. Geol. Geophys.* **Report 166**.

Veevers, J.J. (2001). *Atlas of billion-year old earth history of Australia and neighbours in Gondwanaland*. GEMOC Press, Sydney, Australia.

Wignall, P.B. (2001). Large igneous provinces and mass extinctions. *Earth Sci. Rev.* **53**, 1–33. https://dx.doi.org/10.1016/S0012-8252(00)00037-4.

Wignall, P.B. (2011). Earth science: Lethal volcanism. *Nature* **477**, 285–286. https://dx.doi.org/10.1038/477285a.

Wignall, P.B., Sun, Y., Bond, D.P.G., Izon, G., Newton, R.J., Védrine, S., Widdowson, M., Ali, J.R., Lai, X., Jiang, H., Cope, H., Bottrell, S.H. (2009). Volcanism, Mass Extinction, and Carbon Isotope Fluctuations in the Middle Permian of China. *Science (80-.).* **324**, 1179–1182. https://dx.doi.org/10.1126/science.1171956.

Zachos, J.C., Dickens, G.R., Zeebe, R.E. (2008). An early Cenozoic perspective on greenhouse warming and carbon-cycle dynamics. *Nature* **451**, 279–283. https://dx.doi.org/10.1038/nature06588.

Zhu, M.Y., Babcock, L.E., Peng, S.C. (2006). Advances in Cambrian stratigraphy and paleontology: Integrating correlation techniques, paleobiology, taphonomy and paleoenvironmental reconstruction. *Palaeoworld* **15**, 217–222. https://dx.doi.org/10.1016/j.palwor.2006.10.016.

(Renne et al., 1998; Zhu et al., 2006; McDougall and Wellman, 2011; Gradstein et al., 2012; Ishikawa et al., 2014)

Figure Captions

Fig. 1 Outcrop map of the Antrim Plateau Volcanics in Western Australia and Northern Territory, and inset across Australia. Sample locations from this study are shown as red circles. Previous geochronological sample locations are shown as yellow stars. Previous studies indicated by their age and publication year are: Bultitude (1972), Hanley and Wingate (2000), Macdonald et al. (2005), Glass and Phillips (2006), Evins et al. (2009) and Jourdan et al. (2014).

Fig. 2 Comparative histogram of all published isotope age data concerning the Kalkarindji CFBP. Uncertainties are quoted at 2σ. All Ar-Ar ages are recalibrated to the decay constants of Min et al. (2000) and referenced against GA-1550 with an age of 99.77 Ma as detailed in Renne et al. (2010). **a)** Bultitude (1972), **b)** Hanley and Wingate (2000), **c)** Macdonald et al. (2005), **d)** Glass and Phillips (2006), **e)** Evins et al. (2009), **f)** Jourdan et al. (2014).

Fig. 3 Chemical Index of Alteration (CIA), Mafic Index of Alteration in oxidising conditions (MIA_O) and Mafic Index of Alteration in reducing conditions (MIA_R) plotted against sample elevation. The five samples of this study (closed symbols), plot < 50 on each index, indicating unweathered samples. Kalkarindji samples (open symbols) collated from previous studies (Glass, 2002; Clark, 2014; Gray, 2014; Marshall, 2015).

Fig. 4 $^{40}Ar/^{39}Ar$ age spectra and weighted averages of ten analyses from five samples of the Antrim Plateau Volcanics. Steps included in plateau age segments are shown in dark grey. Analyses rejected from weighted average are shown as red error bars and plagioclase (orange diamonds) and matrix spots (purple circles) are highlighted. The calculated age is shown in green.

Fig. 5 $^{36}Ar/^{40}Ar$ – $^{39}Ar/^{40}Ar$ Inverse isochrones of ten analyses from five samples of the Antrim Plateau Volcanics.

Fig. 6 A comparison between the previously published data, the accepted Early-Middle Cambrian extinction (EMC), a composite δ13C curve (Zhu et al., 2006; Ishikawa et al., 2014) and the results of this study, with analyses from the APV labelled by sample name. a) Bultitude (1972), b) Hanley and Wingate (2000), c) Macdonald et al. (2005), d) Glass and Phillips (2006), e) Evins et al. (2009), f) Jourdan et al. (2014), g) this study, h) minimum age of the EMC boundary (Harvey et al., 2011), i) maximum age of the EMC boundary (Landing et al., 1998). Stratigraphic ages provided by Gradstein et al. (2012).

Table Captions

Table 1 Recalibration of published $^{40}Ar/^{39}Ar$ data to the standardised Min et al. (2000) decay constant and standard values calculated by Renne et al. (2010) as used in this study. Glass and Phillips (2006) and Evins et al. (2009) originally calibrated to Steiger & Jäger (1977) and Renne et al. (1998); Jourdan et al. (2014) originally calibrated to Renne et al. (2011) and Jourdan and Renne (2007).

Table 2 $^{40}Ar/^{39}Ar$ dating results for samples from the Antrim Plateau Volcanics.

Table 3 Isochron data summary.

Table 4 Four weighted average ages of samples from the Antrim Plateau Volcanics; three samples from this study and *LB011* analysed by Glass and Philips (2006).

Table 1

Author	Glass & Phillips (2006)			Evins et al. (2009)	Jourdan et al. (2014)
Sample	HS002(1)	HS002(2)	LB011	EMP 1255	07THD-002
Standard	GA-1550				FCs
Decay Constant (λ)	5.543×10^{-10} a^{-1}				5.5545×10^{-10} a^{-1}
Standard Age (Ma)	98.790 ± 0.540				28.294 ± 0.036
Sample Age (Ma)	**507.5 ± 1.6**	**506.0 ± 2.0**	**504.7 ± 2.2**	**504.6 ± 2.5**	**510.0 ± 4.0**
	Recalibrated to Min et al. (2000) and Renne et al. (2010)				
Decay Constant (λ)	5.463×10^{-10} a^{-1}				
Standard Age (Ma)	99.769 ± 0.108				28.305 ± 0.036
Sample Age (Ma)	**512.8 ± 1.6** [2σ]	**511.3 ± 2.0** [2σ]	**509.9 ± 2.2** [2σ]	**509.6 ± 2.5** [2σ]	**511.0 ± 4.0** [2σ]

GA-1550 = Mount Dromedary biotite (McDougall and Wellman, 2011)
FCs = Fish Canyon sanidine (Renne et al., 1998)

Table 2

Sample	Location	Elevation (m AOD)	Age (Ma)	% ^{39}Ar included	MSWD	Analysis (Instrument)
LB1-970-975(1)	17°25'00.0"S 129°22'37.7"E	1	508.0 ± 8.1 [2σ]	70	0.4	SH (MAP)
LB1-970-975(2)			no plateau			SH (Nu)
LB1-955-960(1)	17°25'00.0"S 129°22'37.7"E	6	499.8 ± 7.0 [2σ]	95.3	1.5	SH (MAP)
LB1-955-960(2)			no plateau			SH (Nu)
BTDF-001(1)	17°00'26.4"S 131°20'44.5"E	134	511.3 ± 5.7 [2σ]	-	1.5	Sp (MAP)
BTDF-001(2)			505.3 ± 6.6 [2σ]	95.2	1.7	SH (MAP)
VCAQ-001(1)	15°23'43.7"S 131°31'27.0"E	198	517.6 ± 7.6 [2σ]	-	0.99	Sp (MAP)
VCAQ-001(2)			no plateau			SH (Nu)
NLBT-006(1)	17°31'22.3"S 129°13'40.4"E	351	411.0 ± 22.0 [95%]	-	9.5	Sp (MAP)
NLBT-006(2)			470.5 ± 8.2 [2σ]	100	1.11	SH (MAP)

MSWD = mean squared weighted deviates.
SH = step-heating, Sp = spot sampling.
MAP = Mass Analyser Products 215-50 noble gas spectrometer, Nu = Nu Instruments Noblesse noble gas spectrometer.

Table 3

Sample	Plateau/Weighted Average Age (Ma)	MSWD	Probability	Isochron Age (Ma)	MSWD	Probability	Initial $^{40}Ar/^{36}Ar$
LB1-970-975(1)	508.0 ± 8.1 [2σ]	0.4	0.880	512.9 ± 7.1	1.8	0.070	336 ± 19
LB1-970-975(2)*	-	-	-	497.9 ± 7.5	25	0.000	295 ± 15
LB1-955-960(1)	499.8 ± 7.0 [2σ]	1.6	0.150	498.6 ± 7.0	1.4	0.200	325 ± 25
LB1-955-960(2)*	-	-	-	496.9 ± 6.6	20	0.000	298 ± 16
BTDF-001(1)	511.3 ± 5.7 [2σ]	1.5	0.092	508.9 ± 8.2	1.6	0.065	302 ± 10
BTDF-001(2)	505.3 ± 6.6 [2σ]	1.7	0.076	504.4 ± 6.6	1.5	0.110	403 ± 51
VCAQ-001(1)	517.6 ± 7.6 [2σ]	0.99	0.460	520.4 ± 56.0	4.4	0.000	317 ± 74
VCAQ-001(2)*	-	-	-	490.2 ± 7.7	4.5	0.000	326 ± 15
NLBT-006(1)	411.0 ± 22.0 [95%]	9.5	0.000	441.0 ± 55.0	9.8	0.000	280 ± 19
NLBT-006(2)	470.5 ± 8.2 [2σ]	1.11	0.350	469.0 ± 9.1	1.2	0.260	304 ± 26

MSWD = mean squared weighted deviates.
*Analysis collected by Nu Instruments Noblesse noble gas spectrometer

Table 4

Sample	Age (Ma)	MSWD	Probability
LB011[a]	509.9 ± 2.2 [2σ]	0.89	0.09
LB1-970-975	502.6 ± 5.5 [2σ]	3.3	0.07
LB1-955-960	498.3 ± 4.8 [2σ]	0.36	0.55
BTDF-001	508.7 ± 4.3 [2σ]	1.9	0.17

MSWD = mean squared weighted deviates.
[a]Glass and Phillips (2006)

Marshall_Ar-Ar_Figure 1

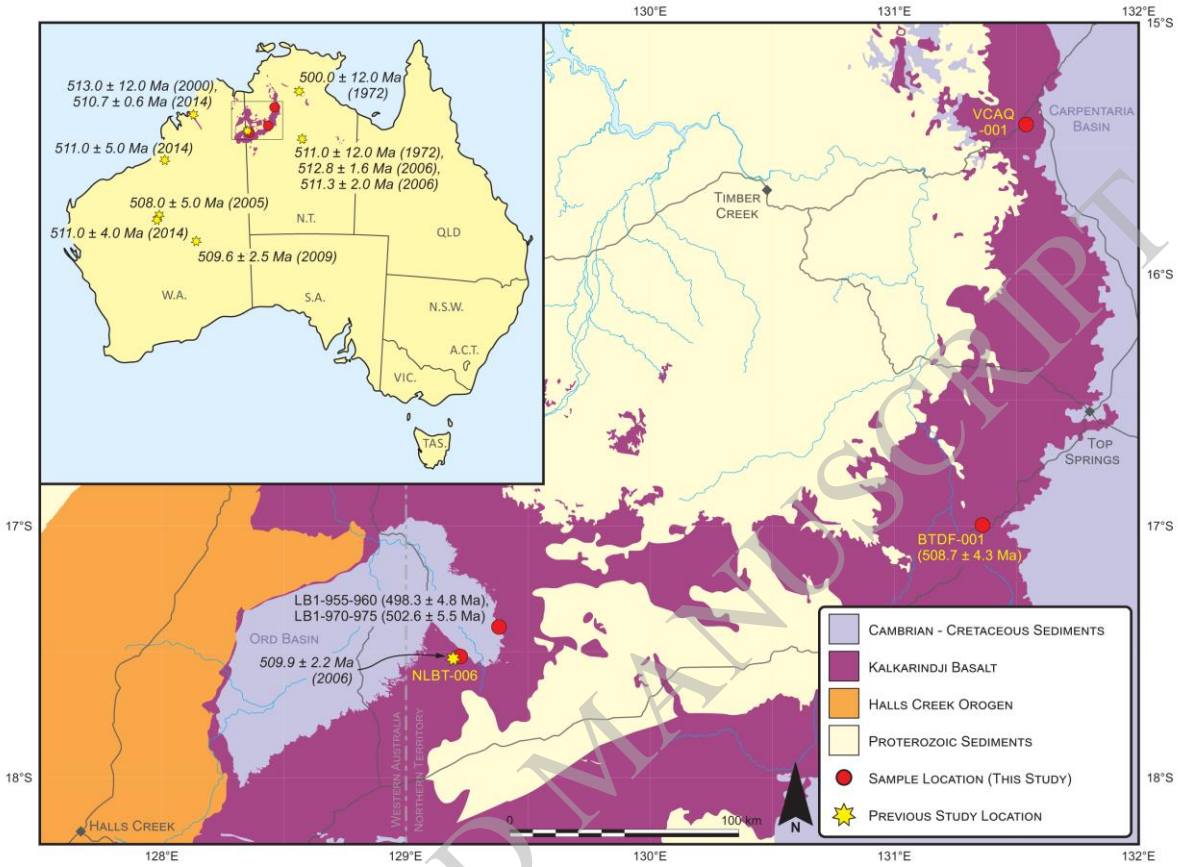

Marshall_Ar-Ar_Figure 2

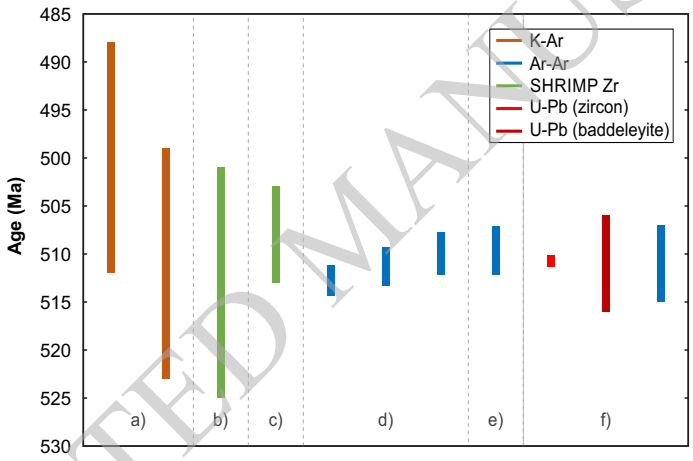

Marshall_Ar-Ar_Figure 3

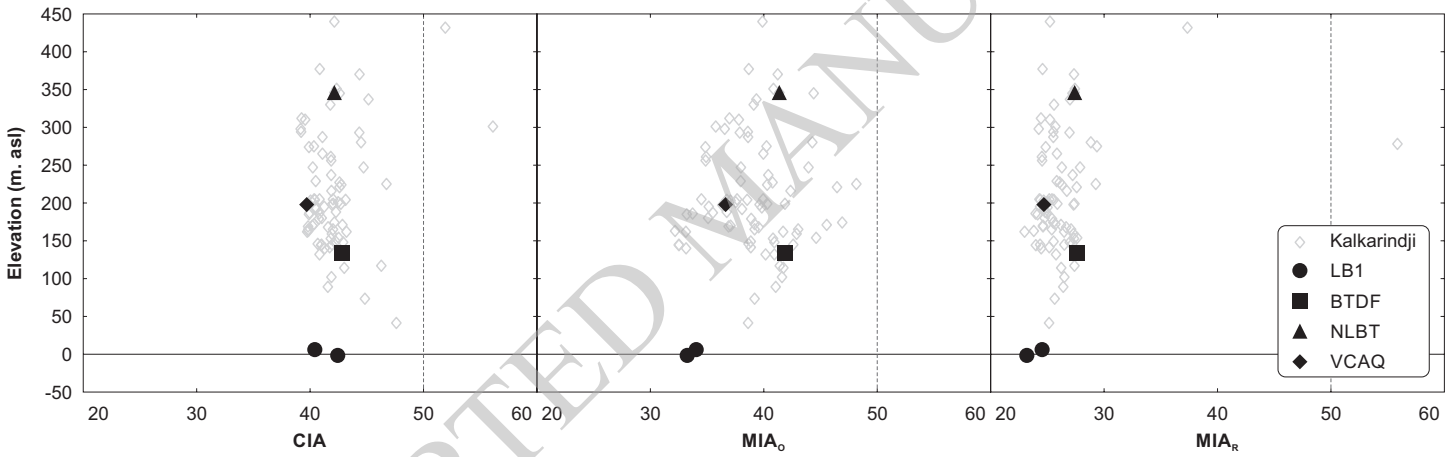

Marshall_Ar-Ar_Figure 4

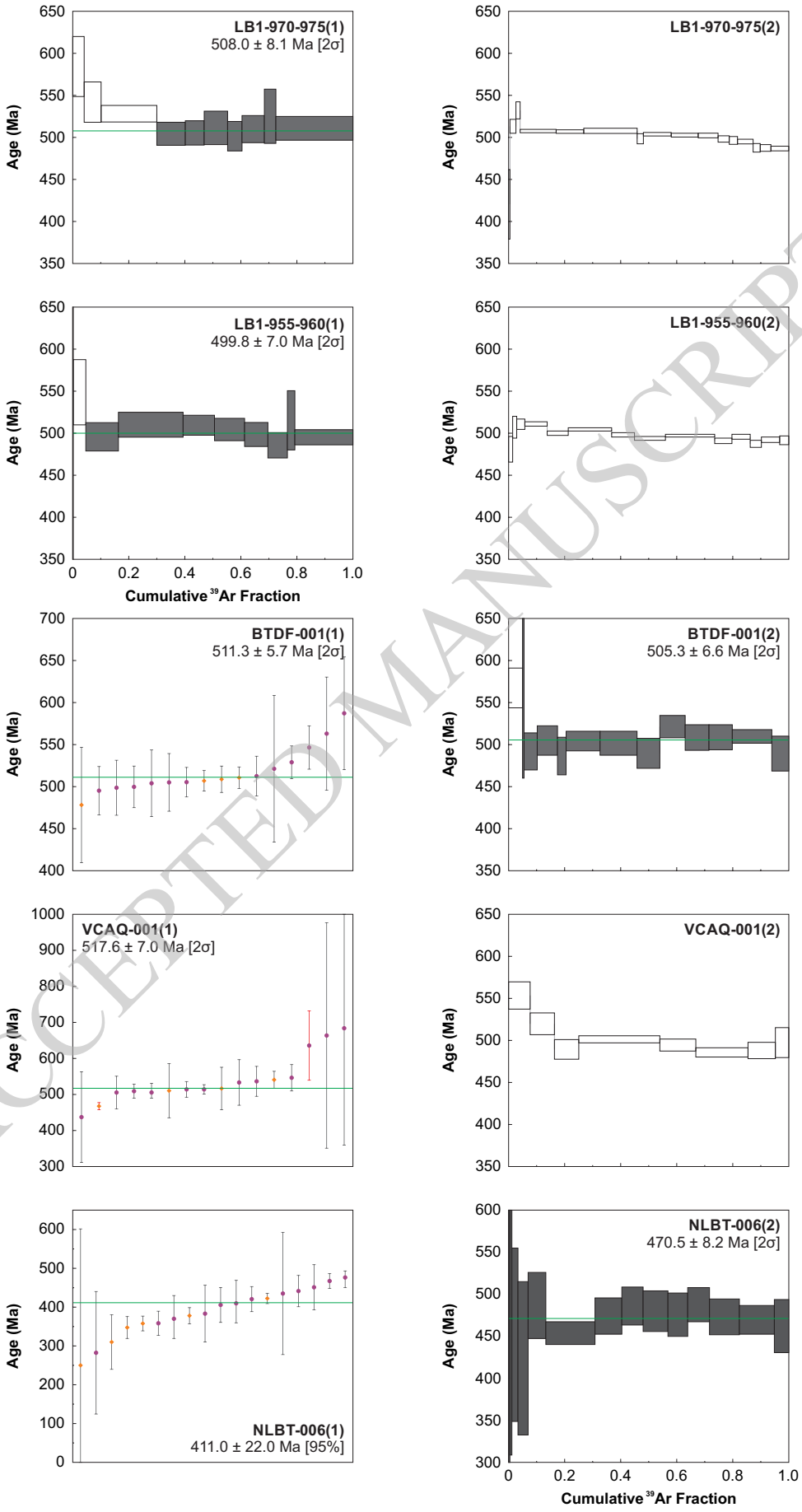

Marshall_Ar-Ar_Figure 5

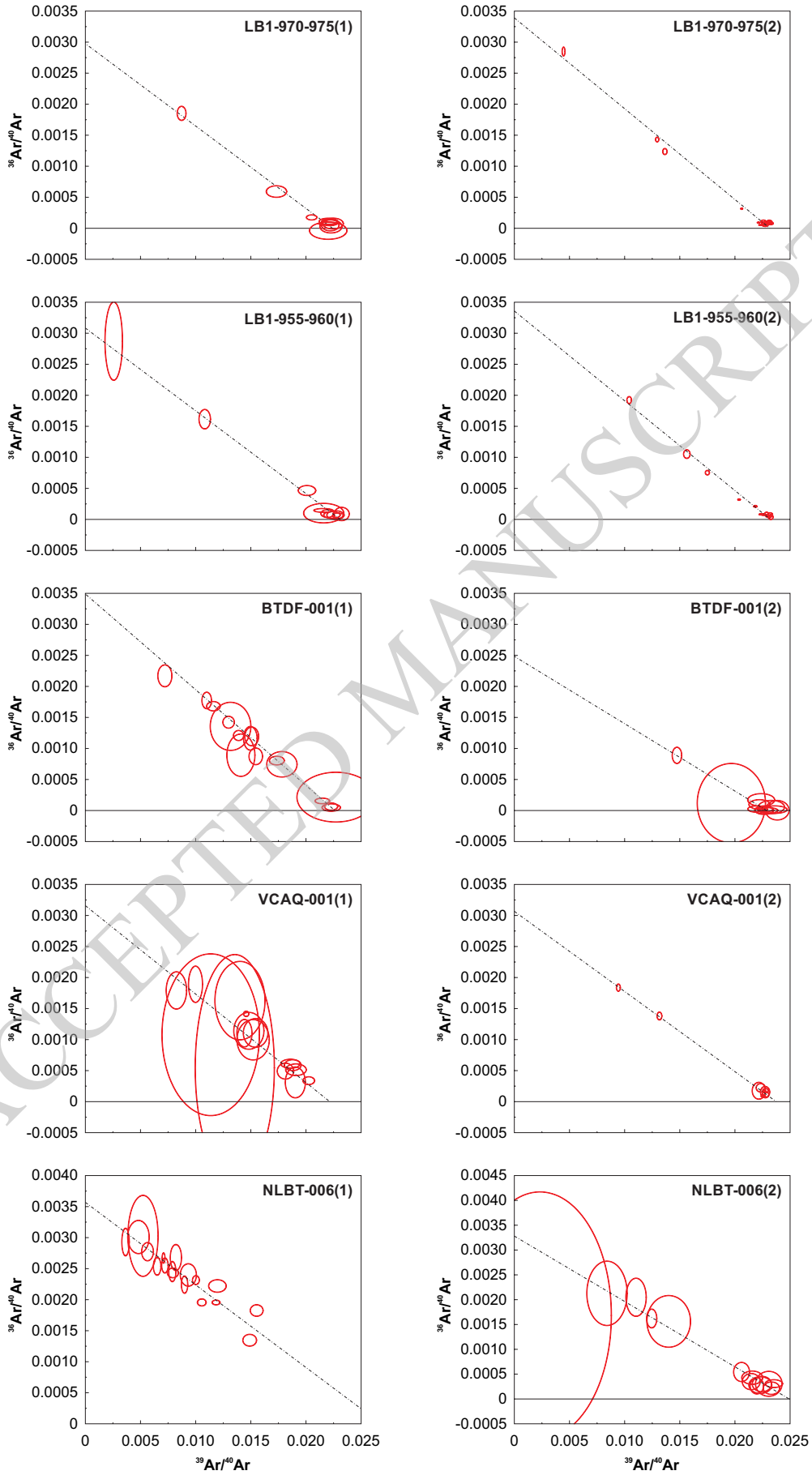

Marshall_Ar-Ar_Figure 6

Chronological order consistent with Figure 2 and Table 1.